A DFT Study of the Mechanism of Palladium-Catalyzed Alkoxycarbonylation and Aminocarbonylation of Alkynes: Hydride versus Amine Pathways

ARTICLE *in* JOURNAL OF ORGANOMETALLIC CHEMISTRY · JUNE 2011

Impact Factor: 2.17 · DOI: 10.1016/j.jorganchem.2011.02.027

3 AUTHORS, INCLUDING:

Rami Suleiman
King Fahd University of Petroleum and Miner…
19 PUBLICATIONS **101** CITATIONS
SEE PROFILE

Bassam El Ali
King Fahd University of Petroleum and Miner…
93 PUBLICATIONS **1,120** CITATIONS
SEE PROFILE

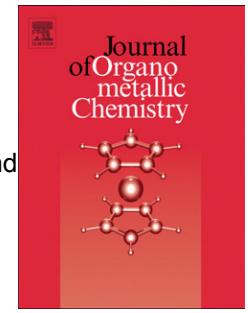

Title: A DFT Study of the Mechanism of Palladium-Catalyzed Alkoxycarbonylation and Aminocarbonylation of Alkynes: Hydride versus Amine Pathways

Authors: Rami Suleiman, Abdelletif Ibdah, Bassam El Ali

PII: S0022-328X(11)00140-9

DOI: 10.1016/j.jorganchem.2011.02.027

Reference: JOM 17017

To appear in: *Journal of Organometallic Chemistry*

Received Date: 20 October 2010

Revised Date: 11 January 2011

Accepted Date: 23 February 2011

Please cite this article as: R. Suleiman, A. Ibdah, B. El Ali. A DFT Study of the Mechanism of Palladium-Catalyzed Alkoxycarbonylation and Aminocarbonylation of Alkynes: Hydride versus Amine Pathways, Journal of Organometallic Chemistry (2011), doi: 10.1016/j.jorganchem.2011.02.027

Synopsis

This theoretical study explores the feasibility and the regioselectivity control of two independent mechanisms: the first is based on the active intermediate $[Pd(II)(P_2)(H)]^+$ (where for the alkoxycarbonylation reaction, and the second is based on the active species $[Pd(II)(P_2)(NR_2)]^+$ for the aminocarbonylation reaction. In hydride cycle, the regioselectivity is mainly determined by the stability of the complex $[Pd(II)(P_2)(COC_3H_5)(CH_3CN)]^+$; however, for the amine cycle, the regioselectivity is determined by the stability of the complex $[Pd(II)(P_2)(C_3H_5CON(CH_3)_2)]^+$.

A DFT Study of the Mechanism of Palladium-Catalyzed Alkoxycarbonylation and Aminocarbonylation of Alkynes: Hydride versus Amine Pathways

Rami Suleiman[a], Abdelletif Ibdah[b], and Bassam El Ali[b*]

[a] *Center of Research Excellence in Corrosion, King Fahd University of Petroleum & Minerals (KFUPM), Dhahran 31261, Saudi Arabia*
[b] *Chemistry Department, King Fahd University of Petroleum & Minerals (KFUPM), Dhahran 31261, Saudi Arabia*

Abstract

A DFT study on the palladium-bisphosphine catalyzed alkoxycarbonylation and aminocarbonylation of alkyne (propyne) is reported. The theoretical study explores the feasibility and the regioselectivity control of two independent mechanisms: the first is based on the active intermediate $[Pd(II)(P_2)(H)]^+$ (where $P_2 = PH_2CH_2CH_2CH_2CH_2PH_2$) for the alkoxycarbonylation reaction, and the second is based on the active species $[Pd(II)(P_2)(NR_2)]^+$ for the aminocarbonylation reaction. The study explains the role of solvent in increasing the yield and in controlling the selectivity of reaction to produce selectively the *trans* isomer in the alkoxycarbonylation reaction (hydride cycle) and the *gem* isomer in the aminocarbonylation reaction (amine cycle). In hydride cycle, the regioselectivity is mainly determined by the stability of the complex $[Pd(II)(P_2)(COC_3H_5)(CH_3CN)]^+$; however, for the amine cycle, the regioselectivity is determined by the stability of the complex $[Pd(II)(P_2)(C_3H_5CON(CH_3)_2)]^+$. The calculations reveal that ligand simplification is not valid in addressing the regioselectivity behavior of alkoxycarbonylation and aminocarbonylation reactions. The kinetic data for the formation of the two key complexes show no difference between the *gem* and *trans* isomers which predict the regioselectivity to be a thermodynamically controlled process.

Keywords: Alkynes, amines, alcohols, bisphosphine, aminocarbonylation, alkoxycarbonylation, hydride, regioselectivity, palladium.

* Corresponding authors. Tel.: +966-3-8604491. Fax: +966-3-8604277

E-mail address: belali@kfupm.edu.sa (B. El Ali)

Introduction

Palladium–catalyzed carbonylation reactions, which are carried out in the presence of various nucleophiles such as amines and alcohols, belong to the most widely used homogenous catalytic reactions in synthetic chemistry [1]. α,β-Unsaturated amides or esters can be prepared by a direct carbonylation of alkynes in the presence of appropriate nucleophiles such as amines (aminocarbonylation) or alcohols (alkoxycarbonylation) (Equation 1).

Equation 1

It is well-known that the ratio of products from aminocarbonylation and alkoxycarbonylation reactions depends strongly on the catalytic system and the reaction conditions employed [2,3]. The development of more efficient catalyst systems in terms of conversion and regioselectivity is still a challenging area for these reactions. However, in order to achieve this goal it is paramount to determine which reaction parameters are the most influential in promoting the formation of highly reactive and stable catalysts [4]. Furthermore, understanding of the regioselectivity profile of these reactions requires an insight on the structure and energy of species involved in these reactions. Recent Progress in computational chemistry has shown that many important chemical and physical properties of the species involved in these reactions can be predicted by various computational techniques [5]. This ability is especially important in these reactions, where the isolation of key intermediates is difficult to achieve. Many catalytic cycles have been proposed for different catalytic systems that catalyze the alkoxycarbonylation [2,6-8] and aminocarbonylation [9-12] of alkynes. The support of these mechanisms was based on the understanding of the influence of different reaction parameters on the catalytic activity and regioselectivity. The use of the theoretical calculations to model catalytic cycles has been reported for metal-catalyzed hydroformylation [13], hydrogenation [14], cross-coupling [15], and other reactions. However, reports on computational studies on the alkoxycarbonylation and aminocarbonylation of alkynes are rare

in the literature. Here, we present a computational study of the alkoxycarbonylation and aminocarbonylation of alkynes that were developed in parallel with experimental results [16]. The aminocarbonylation and alkoxycarbonylation reactions of terminal alkynes took place smoothly and efficiently using the catalyst system $Pd(OAc)_2$/dppb/*p*-TsOH/CH_3CN/CO. The catalytic system was tested and optimized using two different nucleophiles: alcohols and amines. The alkoxycarbonylation reaction produced the *trans* unsaturated ester **4** as a predominant product (90%) with excellent reaction rate, while *gem* isomer was the major amide product **3** (97%) in aminocarbonylation reaction. The catalytic activity and regioselectivity of the two reactions were highly sensitive to the type of solvent, where acetonitrile was the best solvent that produced the highest yield and selectivity of the desired products. Based on experimental results, we are proposing two different catalytic cycles for alkoxycarbonylation (palladium-hydride) and aminocarbonylation (palladium-amine) reactions. The aim of DFT investigation of the two mechanisms is to validate the solution-based observations, to predict the possible key intermediates and transition states, and to address the origin of the change in the rate and regioselectivity of these two reactions.

Computational Details

All calculations were performed using the GAUSSIAN 03 series of programs [17], using the B3LYP functional [18,19]. The structures of the reactants, intermediates, transition states, and products were fully optimized in the gas phase without any symmetry restrictions. The effective core potential [20] and its associated double-ζ LANL2DZ [17,21] basis set were used for the palladium atom. Hydrogen atoms were represented by the 6-31G basis set and the extra series of p-polarization were added for hydride atoms and H atoms involved the in hydrogenation processes. C, N, and O atoms were represented by the 6-31G(d) basis set [22-24]. The frequency calculations and ZPE, which uses the same level of theory and basis set,

were also carried out to determine if the optimized structures were minima or transition states. The validity of each reaction path was further examined by the intrinsic reaction coordinate calculations (IRC). Zero-point energy corrections (ZPE), derived from the frequency calculations, were added to the total energies of each species in the catalytic cycles. The Gibbs energies (*G*) were also calculated at 298.15 K. Solvent effects were taken into account by means of PCM (acetonitrile, ε = 36.64) single-point calculations at the gas-phase optimized geometries [27, 28]. GePol model was employed to construct the solute cavity.

For the DFT study, chelating phosphines based on dhpb ($PH_2CH_2CH_2CH_2CH_2PH_2$) (P_2) and propyne were considered. Methanol is adopted as a nucleophile in the alkoxycarbonylation mechanism and dimethylamine in aminocarbonylation study. The results map the appropriate transition states and associated energy barriers in both the gas phase and acetonitrile [via a polarizable continuum model (PCM)].

Results and Discussion

1. Hydride Cycle

The proposed hydride cycle for the alkoxycarbonylation of propyne is shown on Scheme 1. The proposed intermediates for *trans* isomer (major product in the alkoxycarbonylation reaction) are shown only in this cycle for simplification.

Scheme 1

1.1 Catalyst generation

The first key step in the mechanism of the alkoxycarbonylation of alkyne is the formation of the 16-electron active catalyst $[Pd(II)(P_2)(H)]^+$ (**1C**) via reaction of $Pd(OAc)_2$, P_2 and HX (*p*-TsOH) [9]. Acetonitrile can coordinate to this species forming intermediate **1C-S**, but this

assumption was not considered further since energy barrier to the next step will be endothermically high (18.0 kcal/mol).

1.2 Alkyne coordination

The optimized structure of **2C** (distorted square pyramidal) showed that the Pd-H bond occupies the equatorial position to the $PdP_2C{\equiv}C$. The Pd–C bond lengths are 2.234/2.463 Å, and they are very close to those reported for the palladium-alkyne intermediates [14]. The C≡C bond length in **2C** (1.235 Å) is also longer than in the free form (1.207 Å), and this elongation can be explained by the donation and back donation interaction model of the frontier molecular orbital [29]. The coordination of alkyne to the precursor **1C** is exothermic (25.6 kcal/mol). Other isomers of **2C** have been drawn and optimized (Pd-H bond is perpendicular to C≡C plane) but they are higher in energy than **2C**, and therefore, we did not consider them further in the remained steps of the catalytic cycle.

Figure 1

1.3 Alkyne insertion

The insertion of terminal alkynes, except for acetylene, into the Pd-H bond can occur in two ways, which are described as *anti*-Markovnikov and Markovnikov additions. Therefore, two types of vinyl complexes, *trans* (**T**) and *gem* (**G**), can be formed. This alkylation reaction was considered as the key step for the regioselectivity [30].

The structures of the two transition states, **2C/3CT-TS** and **2C/3CG-TS**, are located and their imaginary vibration modes (409i and 383i cm^{-1}) indicate the migratory insertion of hydrogen to the C≡C triple bond with the shortening of the H-C distances (1.848 and 1.849 Å). The skeleton of **2C/3CT-TS** and **2C/3CG-TS** around the palladium center has a distorted square planar geometry, and the H–Pd–C≡C torsion angles in **2C/3CT-TS** and **2C/3CG-TS** are -0.075° and -0.72°. Taking **2C** as the starting point, the computed activation free energies for

both pathways are 0.4 and 1.7 kcal/mol, respectively. Therefore, there is no kinetic control over the regioselectivity, and this is in agreement with findings for the olefin insertion process of the propene and acetamide complexes [31] and with our published results [16].

Figure 2

The optimized geometries of **3CT** and **3CG** are similar to **1C** in which the PdP_2C forms a distorted triangle or a distorted square planar with a vacant site on palladium center for further molecule coordination. The vinyl moieties in the two geometries are on the same plane with the carbon atoms of dhpb. The *trans* isomer **3CT** is slightly more stable than **3CG** (difference is 1.0 kcal/mol), which indicates that there is no contribution of alkyne insertion step in accounting the regioselectivity of the alkoxycarbonylation reaction. It is worth mentioning that energy difference of about 1 kcal/mol is in the range of the known accuracy limitations of the computational method used in this study.

Figure 3

Since solvent has a crucial role in determining the regioselectivity of the alkoxycarbonylation reaction, especially the role of acetonitrile as a solvent in producing the *trans* isomer in high regioselectivity, we have considered the solvation and coordination properties of acetonitrile in accounting for the interesting regioselectivity of alkoxycarbonylation reaction in this solvent. The calculation of energy profile of the two isomers **3CT** and **3CG** in acetonitrile using PCM resulted in further stability of **3CT** over **3CG** by 1.5 kcal/mol, while solvent coordination by one molecule of acetonitrile (**3CT-S** and **3CG-S**) resulted in comparable energy of the two isomers in gas phase and slight extra stability for the *gem* isomer **3CG-S** in acetonitrile.

Figure 4

1.4 CO Addition and insertion

The following step in the catalytic cycle is the CO addition on the coordinatively unsaturated intermediates $(C_3H_5)PdP_2$ (**3CT/3CG**) to produce the 16-electron saturated species $(C_3H_5)PdP_2(CO)$ (**4CT/4CG**), followed by the insertion (carbonylation) process leading to the corresponding acyl complexes $(C_3H_5CO)PdP_2$ (**5CT/5CG**). The two isomers are isoenergetic with energy difference <0.5 kcal/mol, which reveals no contribution of this step in controlling the regioselectivity of the alkoxycarbonylation reaction. It is worth mentioning that the theoretical calculations reported on the hydroformylation reaction of propene using $HCo(CO)_3$ catalyst accounted the regioselectivity behavior of the hydroformylation reaction based on energy difference between isomers obtained from CO addition step [32]. This step in our system is exothermic for the two isomers **4CT** and **4CG** and our attempts to locate corresponding transition states (**3CT/4CT-TS** and **3CG/4CG-TS**) were failed due to very low barrier of this step [31].

The next step is the CO insertion process converting the vinyl complexes **4CT**/**4CG** into the acyl complexes **5CT**/**5CG**. The optimized geometries of the two isomers showed an interesting rotation of the α,β-unsaturated acyl group to allow η2-coordination of the double bond to the palladium center. The Pd-CO-C angle in **5CT** and **5CG** is 78° and 74° which are much smaller than mono coordinated α,β-unsaturated acyl group (121°). Moreover, the double bond in **5CT** and **5CG** is not coplanar with PdP_2 plane and the distances between Pd and C=C in **5CT** and **5CG** are 2.291/2.436 and 2.240/2.272 Å, respectively. The difference in energy for the two complexes is very small (0.1 kcal/mol), which indicates again the absence of any contribution of this step in accounting for the regioselectivity of the alkoxycarbonylation reaction. The insertion of CO on Pd-vinyl bond is exothermic for the two isomers **5CT** and **5CG** with 7.2 and 7.1 kcal/mol, respectively.

Figure 5

Figure 6

In addition to the adducts and products, we have also investigated the corresponding transition states. This process is well studied at various levels of theory [5]. The transition states **4CT/5CT-TS** and **4CG/5CG-TS** are optimized and characterized by a decrease in the C_3H_5-Pd-CO angle to 57° and 55° in **4CT/5CT-TS** and **4CG/5CG-TS**, respectively. The negative direction modes of the above transition states (283i and 306i) indicate the right direction of carbonylation. The computed carbonylation barriers for both the *trans* (**4CT**→(**4CT/5CT-TS**)→ **5CT**) and the *gem* routes (**4CG**→(**4CG/5CG-TS**)→ **5CG**) are 5.9 and 8.2 kcal/mol, and they are close to those of corresponding step in propene hydroformylation [30].

Figure 7

1.5 Solvent coordination

Since acetonitrile solvent showed experimentally an interesting role in the regioselectivity of the alkoxycarbonylation of propyne reaction to favor the formation of the *trans* isomer, the coordination of CH_3CN molecule to intermediates **5CT** and **5CG** has been studied. The skeleton around the palladium center for the resulted isomers **6CT** and **6CG** is a distorted square planar and the PPdN≡C angle in **6CT** and **6CG** is 171°. The Pd-N distance in **6CT** and **6CG** is 2.160 and 2.163 Å, respectively. Moreover, solvent coordination to **5CT** and **5CG** is computed to be highly exothermic by 16.9 and 12.2 kcal/mol, and the difference in the thermodynamic stability of the products from this high exothermic addition (**6CT** and **6CG**) could be responsible for the observed regioselectivity. This clearly described the high regioselectivity towards the *trans* ester using acetonitrile as a solvent [16]. This initial result on the role of acetonitrile solvent in controlling the regioselectivity of the alkoxycarbonylation reaction encouraged us to consider in future computational studies the effect of coordination and solvation properties of other solvents.

Figure 8

1.6 Methanol oxidative addition and α,β-unsaturated ester reductive elimination

The starting points of this step are isomers obtained from the carbonylation and solvent coordination processes (**6CT** and **6CG**). The coordination of methanol leads to the formation of the two isomers **7CT** and **7CG**. It is worth mentioning that isomers **7CT** and **7CG** can be obtained directly from the coordination of methanol to isomers **5CT** and **5CG**. However, the presence of catalytic amounts of methanol versus large availability of acetonitrile molecules in the reaction media and the interesting regioselectivity of alkoxycarbonylation reaction encouraged us to propose the formation of isomers **6CT** and **6CG**. It is interesting to note also that the H–O bonds in **7CT** and **7CG** are parallel to the Pd–C_{acyl} bonds. One reason for this conformation in **7CT** and **7CG** is the attractive electrostatic interaction (H-bonding) between the polar H–O bond and the acyl C=O bond. The H⁻O distances in **7CT** and **7CG** are 1.993 and 2.088 Å, while the Pd-O distances are 2.239 and 2.242 Å

Figure 9

For the oxidative addition, the attempts to determine the corresponding intermediates (the hydride and methoxy complex) from the addition of methanol were unsuccessful. The optimization following the negative vibration modes leads to the formation of intermediates **8CT** and **8CG** directly without any barrier. This indicates that the potential energy surface is flat. The driving force for the simplified reaction might be the attractive electrostatic interaction between the negatively charged oxygen of the CH_3O ligand and the positively charged carbon center of the acyl ligand; both ligands already have the appropriate orientation, which can facilitate further reaction [31].

On the basis of the most stable acyl intermediates (**5CT** and **5CG**), the coordination of CH_3OH is exothermic by 11.9 and 8.9 kcal/mol for **7CT** and **7CG**. Since it is not possible to determine the corresponding intermediates of the oxidative addition, and the subsequent

transition states for the reductive elimination, no energetic data for these species are available. From the CH_3OH adducts, the formation of the ester complex **8CT/TEP** is exothermic by 2.6 kcal/mol and endothermic by 1.3 kcal/mol for **8CG/GEP**. Taking **2C** and (CO + CH_3OH) as the starting point, the formation of the separated product and **1C** are exothermic for the *trans* and *gem* esters by 50.3 and 49.3 kcal/mol, respectively.

Figure 10

The calculated relative energies for *trans* isomer intermediates in the alkoxycarbonylation of propyne in the gas phase are shown in Scheme 2.

Scheme 2

1.7. Solvation effect

The effect of acetonitrile, as a solvent, has been studied using a polarizable continuum solvent model (PCM). This process yielded results that were similar to those already discussed for the gas phase. Thus, no significant changes in the values of the relative energies do take place and no substantive changes in the energy profiles except for the alkyne coordination step, which is an exothermic process by a 10.2 kcal/mol in acetonitrile. Interestingly, some of the energy barriers are actually higher when the continuum solvent model is applied. The most remarkable corresponding to the change **4CT→4CT/5CT-TS** and **4CG→4CG/5CG-TS**, which are 5.9 and 8.2 kcal/mol in the gas phase versus 6.5 and 9.2 kcal/mol in acetonitrile. The difference in relative energies between *trans* and *gem* intermediates slightly changed for initial intermediates in the catalytic cycle. The energy difference between intermediates **4CT** and **4CG** increased from a 0.5 kcal/mol in gas phase to a 1.0 kcal/mol in acetonitrile. Interestingly, an opposite case was found with intermediates **7CT** and **7CG**, where the energy difference dropped from a 3.0 kcal/mol in gas phase to a 0.7 kcal/mol in acetonitrile. Nevertheless, the regioselectivity profile in acetonitrile showed the same energy difference between intermediates **6CT** and **6CG,** as key intermediates in

accounting for the regioselectivity of the alkoxycarbonylation reaction. The computed energetic data for the whole reactions in hydride-cationic cycle are available in supporting information (Table S1).

1.8. Test of validity of ligand simplification

Ligand simplification implied in the theoretical calculations was necessary to minimize the time of computation. Successful interpretation of many physical and chemical properties of catalytic species was computationally successful using this simplification [14]. However, since regioselectivity profile of alkoxycarbonylation and aminocarbonylation of alkynes are affected much by the steric and electronic properties of ligands [16], we have decided to test the validity of ligand simplification in the present calculations. The simplification has been removed from all *trans* intermediates **3CT**, **4CT**, **5CT**, **6CT**, **7CT** and **8CT** and their corresponding *gem* isomer intermediates plus intermediates **1C** and **2C** for accurate comparison with the results of the simplified intermediate.

Data shown in Table 1 prove a great effect of the ligand simplification on the energy difference between *trans* and *gem* intermediates in the hydride cycle. All *trans* intermediates are now more stable than their corresponding *gem* intermediates (after removing ligand simplification) in the gas phase and this stability was further increased in acetonitrile. These results gave further approval for obtaining *trans* ester regioselectively via hydride cycle.

Remarkably, the energy profile of elementary steps involved in the hydride cycle changed significantly for the initial non-simplified intermediates and less significant change was observed for the late intermediates. Based on the above results, we believe that ligand simplification is not valid in theoretical calculations targeting a specific explanation of energy profile of our proposed catalytic cycle or in accounting for the origin of regioselectivity profile.

The comparison of the energy profile of all elementary steps in the cationic cycle between simplified and non-simplified *trans* intermediates in gas phase and acetonitrile is shown in Table 2.

Table 1

Table 2

2. Amine cycle

Based on the earlier published experimental results for the aminocarbonylation of terminal alkyne [16], we have proposed a catalytic cycle that involves a palladium-amine active species to afford eventually the *gem* amide as a predominant product. The theoretical calculations based on the palladium-amine mechanism for the aminocarbonylation of terminal alkynes have not been yet reported in literature, which encouraged us to carry out a first simple computation on a simplified proposed palladium-amine mechanism for the aminocarbonylation of propyne (Scheme 3). The mechanism involves: (i) the formation of an amide-palladium complex generated by the insertion of CO into a Pd-N bond, (ii) the migration of the amide moiety on a carbon atom of the triple bond of the propyne π-coordinated to the metal center, and (iii) the protonoylsis of the resulted vinyl intermediate. In this mechanism, the regioselectivity of the reaction can be determined by comparing the thermodynamic stability of only one intermediate for each isomer (**5AT** and **5AG**), unlike hydride mechanism discussed above. It is worth noting that our calculations based on the hydride cycle as a pathway for the aminocarbonylation reaction were not successful in explaining the regioselectivity in the aminocarbonylation reaction. The replacement of the alkoxy group in intermediates **6CT**, **6CG** and the subsequent intermediates in the hydride cycle by any amine as a nucleophile still showing higher stability for *trans* over *gem* amide intermediates, and this disagrees with our experimental results published earlier for the aminocarbonylation reaction [16].

Scheme 3

2.1. Catalyst generation

The first key step in the alkoxy-mechanism of the alkoxycarbonylation of alkyne is the formation of the 16-electron active catalyst $[Pd(II)(P_2)(NMe_2)]^+$ (**1A**) via reaction of $Pd(OAc)_2$, P_2 and $HNMe_2$ [33,34]. The optimized geometry of this species around palladium center is a distorted tringle with P-Pd-N angles of 106° and 159°, and Pd-P bonds distance of 2.294 and 2.392 Å.

2.2. CO Coordination

The next step is the CO coordination to **1A**. The structure of the resulting optimized geometry **2A** is a square distorted planar conformation around the central palladium with C-Pd-N angle of 95° and Pd-N bond distance of 2.089 Å. These data are in agreement with X-ray data reported in the literature for palladium-diphosphine-ammine complexes [34]. The computed relative energy of **2A** reveals that this step is exothermic by a 9.1 kcal/mol.

Figure 11

2.3. CO Insertion

The insertion of CO in **2A** will leads to the formation of palladium-amide intermediate **3A**. The P-Pd-C-N dihedral angles are 1° and 179° making the geometry around central palladium approaching a planar distorted triangle shape. Palladium-amide intermediates have been proposed before in the aminocarbonylation of internal alkynes [12]. The calculated energy for this insertion step is exothermic by 24.1 kcal/mol, which suggests a higher stabilizing energy as compared to the stabilization energy obtained from CO insertion into Pd-C bond in the hydride cationic cycle (see 1.4). The transition state for this insertion step (**2A/3A-TS**) has been also located.

2.4. Alkyne coordination and insertion

The coordination of alkyne on palladium occurs with bidentate coordination of dppb ligand (**4A**) or can be accompanied by dechelation of one Pd-phosphine ligand yielding **4A-1**. The energies of the two optimized geometries are much different and the bidentate phosphine ligand in **4A** is more stable than monodentate one in **4A-1** by a 15.7 kcal/mol, and, therefore, **4A** will be adopted in this study.

Figure 12

The next step is the migration of the amide moiety to the carbon atom of the triple bond of the propyne. Again, this migration can occur in two ways, *anti*-Markovnikov and Markovnikov additions yielding *trans* (**5AT**) and *gem* (**5AG**) isomers, respectively. The optimized geometry for the two isomers shows an interesting coordination of the lone pair of electrons of the alcohol's oxygen atom to palladium center leading to the formation of planar five-membered ring. The migration step is highly exothermic for the two isomers **5AT** and **5AG** by 18.1 and 21.1 kcal/mol, respectively. This difference in thermodynamic stability for **5AG** over **5AT** can be also used to explain the regioselectivity of the alkoxycarbonylation reaction to produce the *gem* isomer as a major product starting from palladium-amine species.

Figure 13

Furthermore, the removal of ligand simplification from the above two key intermediates increased the stability of **5AG-LNS** over **5AT-LNS** by 7.2 kcal/mol in gas phase and 6.2 kcal/mol in acetonitrile. The above results gave more support for the great role of the type of solvent and ligand towards the formation of palladium-hydride or palladium-amine species, and hence different regioselectivity profiles for the alkoxycarbonylation and aminocarbonylation reactions.

Figure 14

It is worth noting that the geometry of the non-simplified regioselectivity key intermediates showed longer Pd-N distance (2.258 Å) than simplified intermediates (2.182 Å), which indicates great effects of the ligand simplification on the energy and regioselectivity profile in the amine cycle intermediates. The computed energetic data for the whole reactions in amine cycle are available in the supporting information (Table S3). Also, the calculated relative energies for *gem* isomer intermediates in the aminocarbonylation of propyne in the gas phase are shown in Scheme 4.

2.5. Solvation effect of amine cycle

The solvation effect of acetonitrile has been studied on amine cycle using PCM model. The relative stability of most intermediates involved in the catalytic cycle was lowered in irregular way by introducing this effect. However, only the key regioselective intermediates **5AG** and **5AT** gained more stability by introducing this effect, however with no change in the regioselectivity profile (**5AG** is more stable than **5AT** by a 2.4 kcal/mol).

The results obtained from the theoretical calculations based on hydride and amine cycles in case of changing the alkyne substrate showed no change in the regioselectivity profiles of the alkoxycarbonylation and aminocarbonylation reactions. These results confirm the experimental results we had reported previously in literature [12].

Conclusions

Theoretical investigations (DFT/B3LYP) of the palladium-hydride and palladium-amine mechanisms, proposed for the alkoxycarbonylation and aminocarbonylation reactions, were carried out to interpret the major differences of the activity and the regioselectivity of the two above mentioned reactions. This study compared the theoretical results with experimental observations, which have already been reported by our group. The results obtained indicate

the formation of *trans* ester isomer via palladium-hydride cycle, while palladium-amine mechanism is the key for the formation of *gem* isomer. The results prove the ligand simplification protocol to be non-valid in this type of investigation. The role of acetonitrile solvent in enhancing the yield and regioselectivity of the alkoxycarbonylation and aminocarbonylation reactions was mainly in improving the stability of catalytic intermediates in the two proposed mechanisms.

Acknowledgments

We thank King Fahd University of Petroleum and Minerals (KFUPM-Saudi Arabia) for providing all support to this project. This project has been funded by King Fahd University of Petroleum and Minerals under project no. CY/Palladium/295.

References

[1] R. Skoda-Földes, L. Kollár, Curr. Org. Chem., 6 (2002) 1097-1119.
[2] S. Akao, K. Sugawara, Y.I. Amino, J. Mol. Cat., 157 (2000) 117-122.
[3] B. El Ali, J. Tijani, A.M. El-Ghanam, J. Mol. Cat., 187 (2002) 17-33.
[4] T.E. Barder, M.R. Biscoe, S.L. Buchwald, Organometallics, 26 (2007) 2183-2192.
[5] S. Niu, M. B. Hall, Chem. Rev., 100 (2000) 353-405.
[6] B. Cornils, W. A. Herrmann, Applied Homogeneous Catalysis with Organometallic Compounds;; Wiley-VCH:Weinheim, (1996).
[7] J. Tijani, R. Suleiman, B. El Ali, Appl.Organomet. Chem., 22 (2008) 553-559.
[8] B. El Ali, H. Alper, J. Mol. Cat., 6 (1991) 29-33.
[9] U. Matteoli, A. Scrivanti, V. Beghetto, J. Mol. Cat., 213 (2004) 183-186.
[10] B. El Ali, J. Tijani, Appl. Organomet. Chem., 17 (2003) 921-931.
[11] Y. Li, H. Alper, Z. Yu, Org. Lett., 8 (2006) 5199-5201.
[12] J.H. Park, S.Y. Kim, S.M. Kim, Y.K. Chung., Org. Lett.,9 (2007) 2465-2468.
[13] C.F. Huo, Y.W. Li, M. Beller, H. Jiao, Organometallics, 22 (2003) 4665-4677.

[14] J. L. Serrano, A. Lledós, S.B. Duckett, Organometallics, 27 (2008) 43-52.

[15] L.J. Goossen, D. Koley, H.L. Hermann, W. Thiel, J. Am. Chem. Soc., 127 (2005) 11102-11114.

[16] R. Suleiman, J. Tijani, B. El Ali, Appl.Organomet. Chem., 24 (2010) 38-46.

[17] M.J. Frisch, G.W. Trucks, H.B. Schlegel, G.E. Scuseria, M.A. Robb, J. R. Cheeseman, J.A. Montgomery, T. Vreven, K.N. Kudin, J.C. Burant, J.M. Millam, S.S. Iyengar, J. Tomasi, V. Barone, B. Mennucci, M. Cossi, G. Scalmani, N. Rega, G.A. Petersson, H. Nakatsuji, M. Hada, M. Ehara, K. Toyota, R. Fukuda, J. Hasegawa, M. Ishida, T. Nakajima, Y. Honda, O. Kitao, H. Nakai, M. Klene, X. Li, E.J. Knox, H.P. Hratchian, J.B. Cross, V. Bakken, C. Adamo, J. Jaramillo, R. Gomperts, R.E. Stratmann, O. Yazyev, A.J. Austin, R. Cammi, C. Pomelli, J.W. Ochterski, P.Y. Ayala, K. Morokuma, G.A. Voth, P. Salvador, J.J. Dannenberg, V.G. Zakrzewski, S. Dapprich, A.D. Daniels, M.C. Strain, O. Farkas, D.K. Mallick, A.D. Rabuck, K. Raghavachari, J.B. Foresman, J.V. Ortiz, Q. Cui, A.G. Baboul, S. Clifford, J. Cioslowski, B.B. Stefanov, G. Liu, A. Liashenko, P. Piskorz, I. Komaroni, R.L. Martin, D.J. Fox, T. Keith, M.A. Al-Laham, C.Y. Peng, A. Nanayakkara, M. Challacombe, P.M.W. Gill, B. Johnson, W. Chen, M.W. Wong, C. Gonzalez, J.A Pople, *Gaussian 03, Revision D.01*; Gaussian, Inc.: Wallingford, CT, (2004).

[18] A.D. Becke, J. Chem. Phys., 98 (1993) 5648-5653.

[19] C. Lee, W. Yang, R.G. Parr, Phys. Rev. B: Condens. Matter Mater. Phys., 37 (1988) 785-789.

[20] P.J. Hay, W.R. Wadt, J. Chem. Phys., 82 (1985) 299-311.

[21] A. Höllwart, M. Böhme, S. Dapprich, A.W. Ehlers, A. Gobbi, V. Jonas, K.F. Köhler, R. Stegmann, A. Veldkamp, G. Frenking, Chem. Phys. Lett.**,** 208 (1993) 237-240.

[22] W.J. Hehre, R. Ditchfield, J.A. Pople, J. Chem. Phys., 56 (1972) 2257-2262.

[23] P.C. Hariharan, J.A. Pople, Theor. Chim. Acta., 28 (1973) 213-222.

[24] M.M. Francl, W.J. Pietro, W.J. Hehre, J.S. Binkley, M.S. Gordon, D.J. DeFrees, J.A. Pople, J. Chem. Phys., 77 (1982) 3654-3666.

[25] R. Seeger, J.A. Pople, J. Chem. Phys., 66 (1977) 3045-3051.

[26] R. Bauernschmitt, R.J. Ahlrichs, Chem. Phys., 104 (1996) 9047-9053.

[27] J. Tomasi, M. Persico, Chem. Rev., 94 (1994) 2027-2033.

[28] C. Amovilli, V. Barone, R. Cammi, E. Cancès, M. Cossi, B. Mennucci, C.S. Pomelli, J.J. Tomasi, Adv. Quantum Chem., 32 (1999) 227-261.

[29] J.A. Serrano, A. Lledós, B. Duckett, Organometallics, 27 (2008) 43-52.

[30] C. Huo, Y.W. Li, M. Beller, H. Jiao, Organometallics, 22 (2003) 4665-4677.

[31] S. Klaus, H. Neumann, H. Jiao, J. Von, A. Wangelin, D. Gördes, D. Strübing, S. Hübner, M. Hateley, C. Weckbecker, K. Huthmacher, T. Riermeier, M. Beller, J. Organometal. Chem., 689 (2004) 3685-3700.

[32] F.E. Hong, Y.C. Chang, Organometallics, 23 (2004) 718-729.

[33] C. Amatore, E. Carre, A. Jutand, M.A. M'Barki, Organometallics, 14 (1995) 1818-1826.

[34] A.L. Seligson, W.C. Trogler, J. Am. Chem. Soc., 113 (1991) 2520-2527.

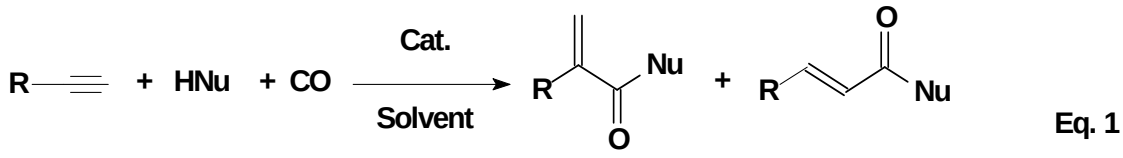

Eq. 1

1 2 3 4

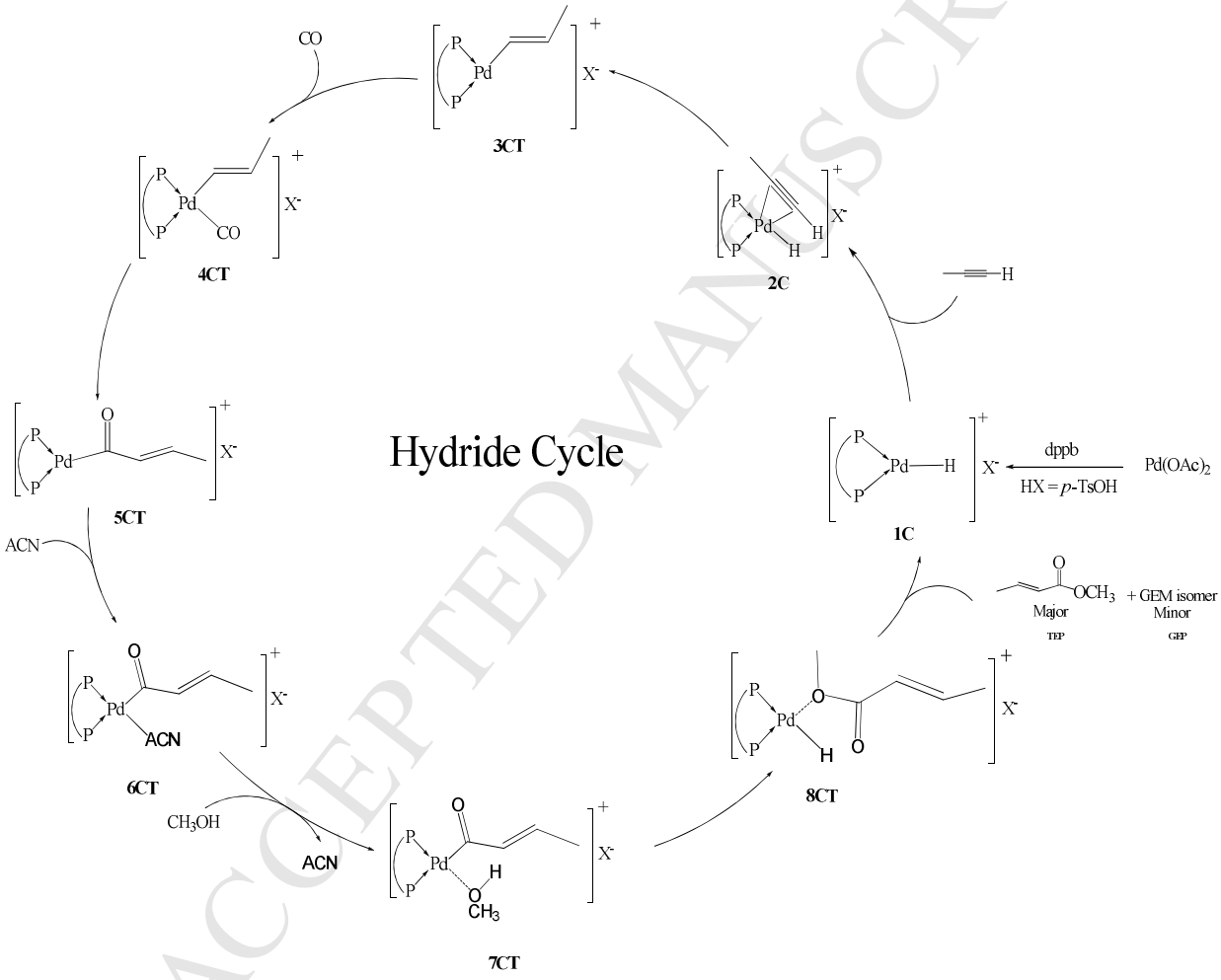

Scheme 1. DFT-derived scheme for alkoxycarbonylation of propyne by a hydride-cationic Palladium(II) bisphosphine complex.

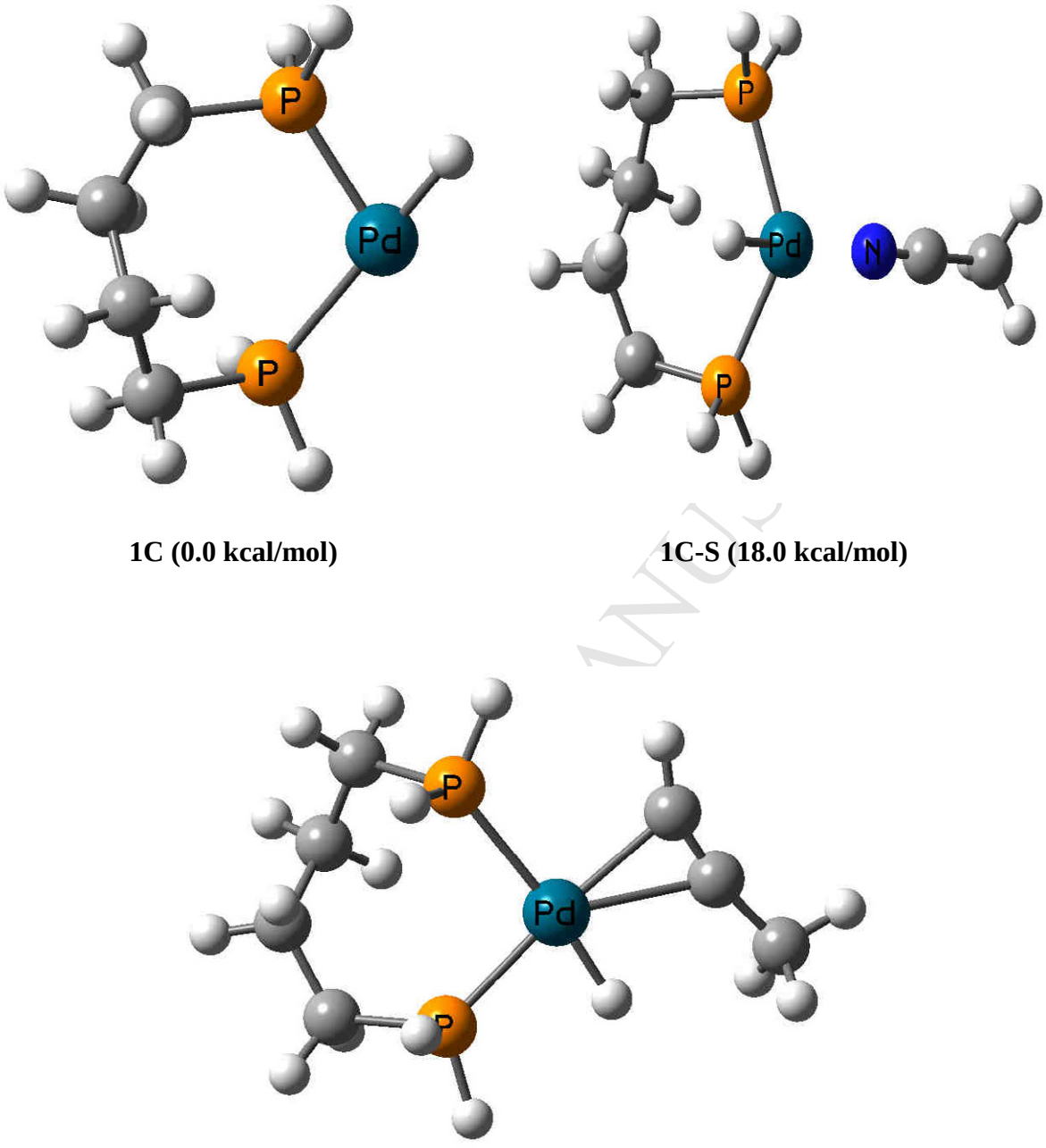

Figure 1. Optimized structures and relative free energies for intermediates **1C**, **1C-S** and **2C**.

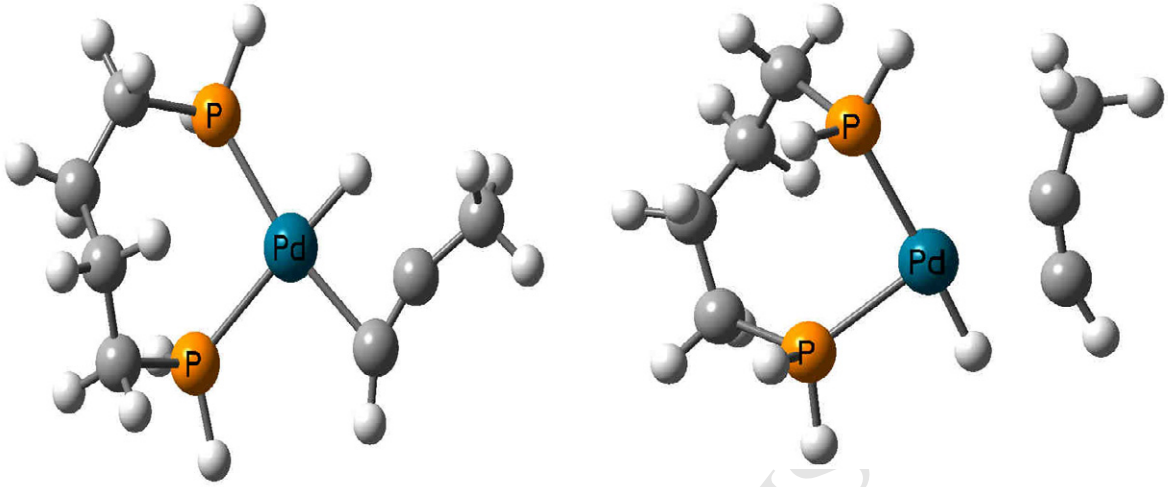

2C/3CT-TS (0.4 kcal/mol) **2C/3CG-TS (1.7 kcal/mol)**

Figure 2. Optimized structures and relative free energies for transition states **2C/3CT-TS** and **2C/3CG-TS**.

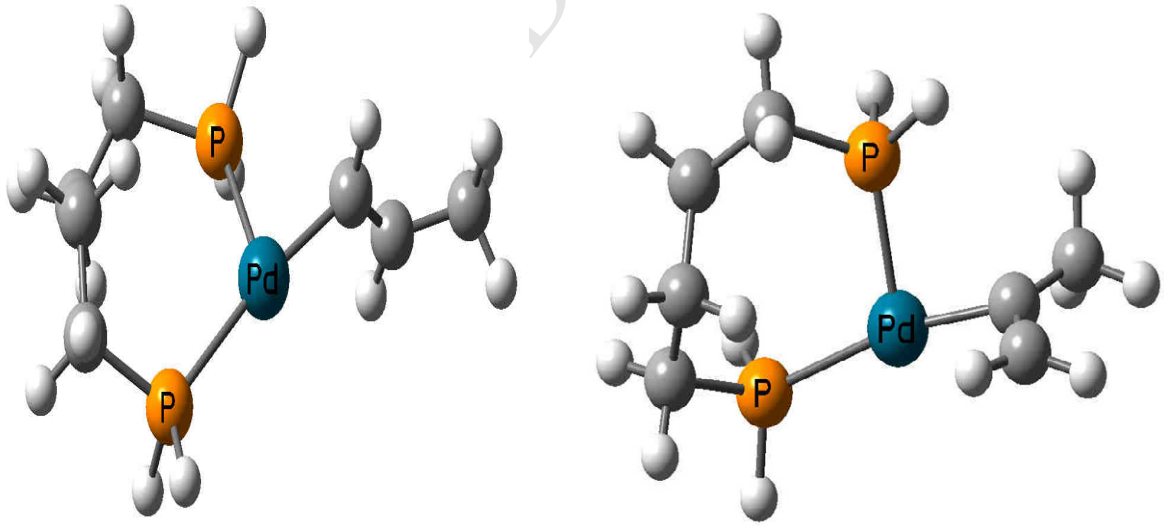

3CT (-14.5 kcal/mol) **3CG (-15.4 kcal/mol)**

Figure 3. Optimized structures and relative free energies for intermediates **3CT** and **3CG**.

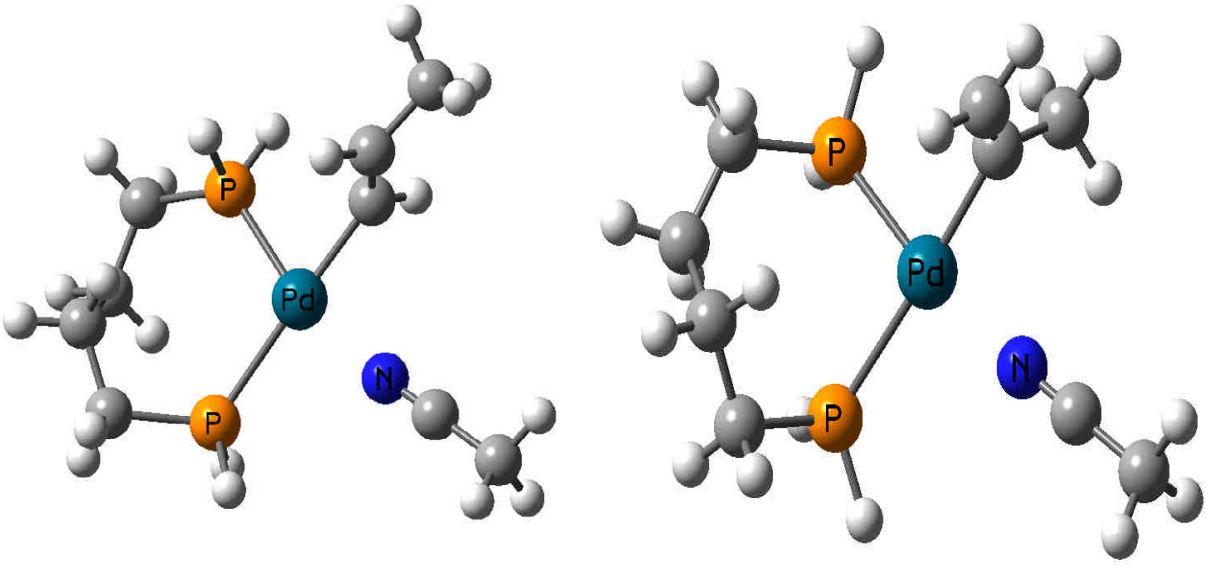

3CT-S (-22.7 kcal/mol) **3CG-S (-23.3 kcal/mol)**

Figure 4. Optimized structures and relative free energies for intermediates **3CT-S** and **3CG-S**.

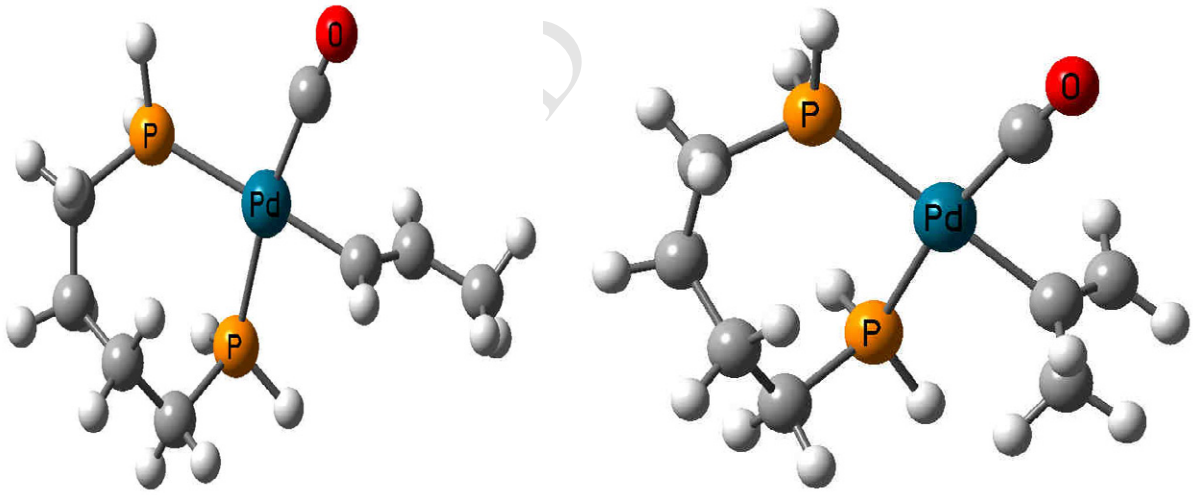

4CT (-19.3 kcal/mol) **4CG (-19.8 kcal/mol)**

Figure 5. Optimized structures and relative free energies for intermediates **4CT** and **4CG**.

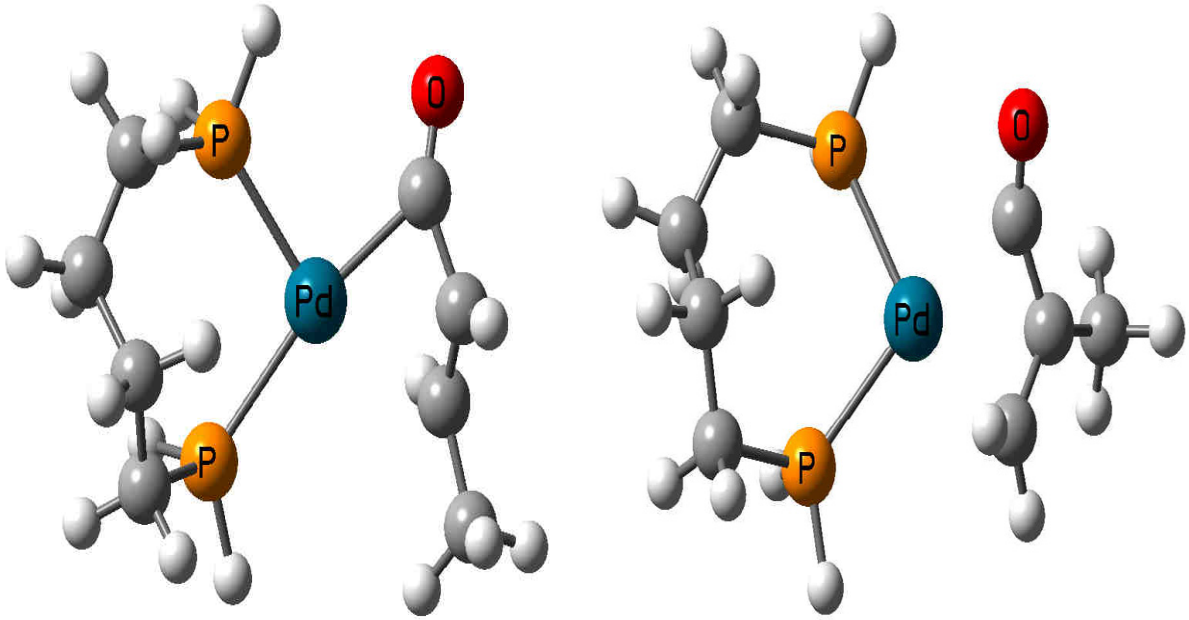

5CT (-26.1 kcal/mol) **5CG (-26.7 kcal/mol)**

Figure 6. Optimized structures and relative free energies for intermediates **5CT** and **5CG**.

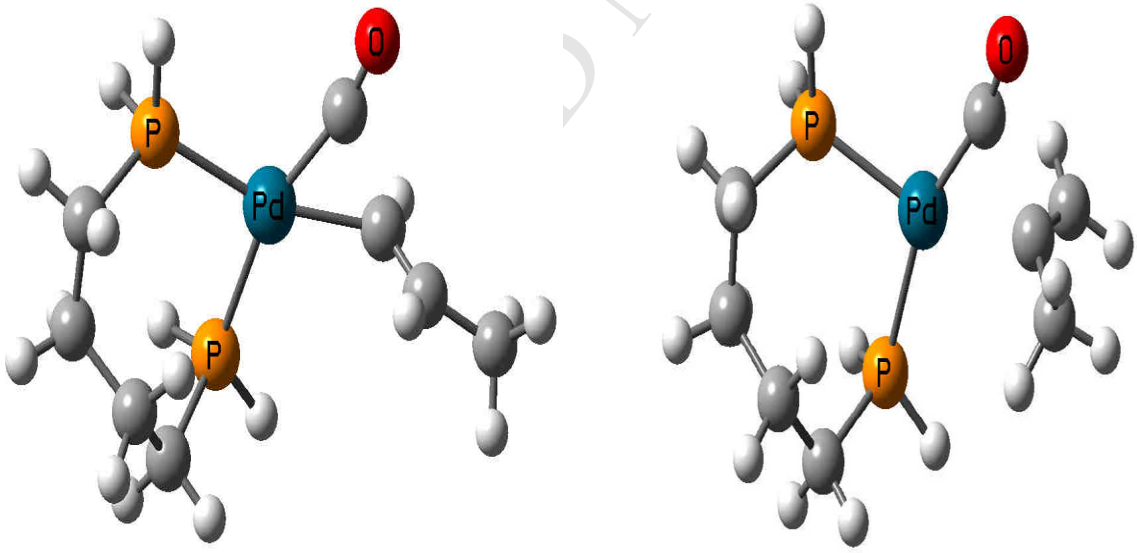

4CT/5CT-TS (5.9 kcal/mol) **4CG/5CG-TS (8.2 kcal/mol)**

Figure 7. Optimized structures and relative free energies for transition states **4CT/5CT-TS** and **4CG/5CG-TS**.

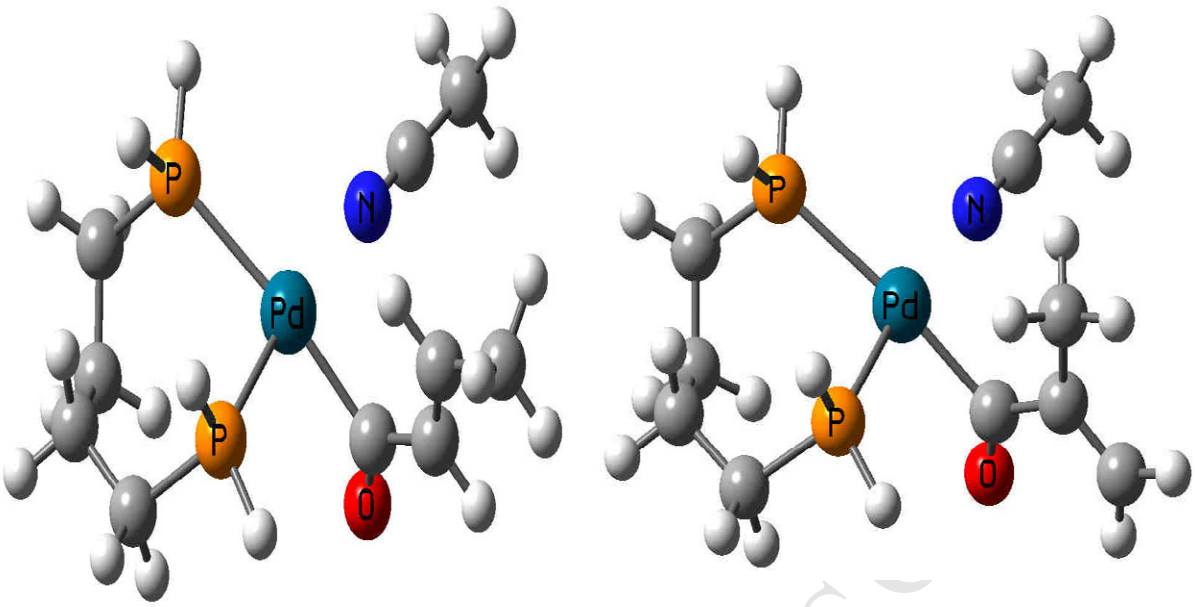

6CT (-16.9 kcal/mol) **6CG (-12.2 kcal/mol)**

Figure 8. Optimized structures and relative free energies for intermediates **6CT** and **6CG**.

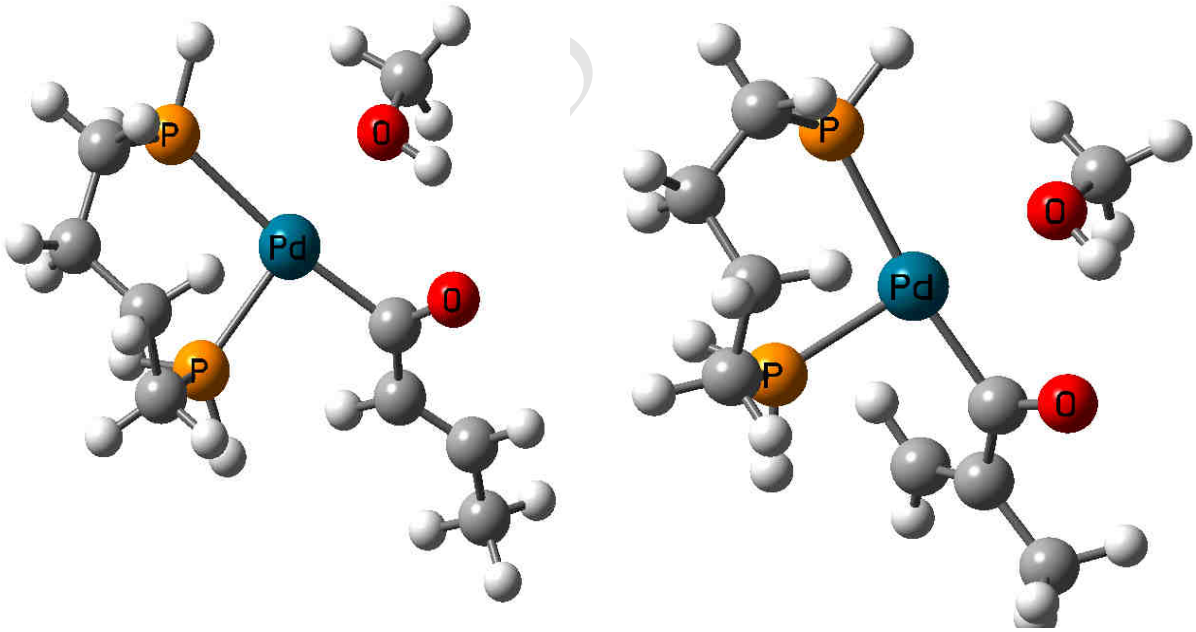

7CT (-11.9 kcal/mol) **7CG (-8.9 kcal/mol)**

Figure 9. Optimized structures and relative free energies for intermediates **7CT** and **7CG**.

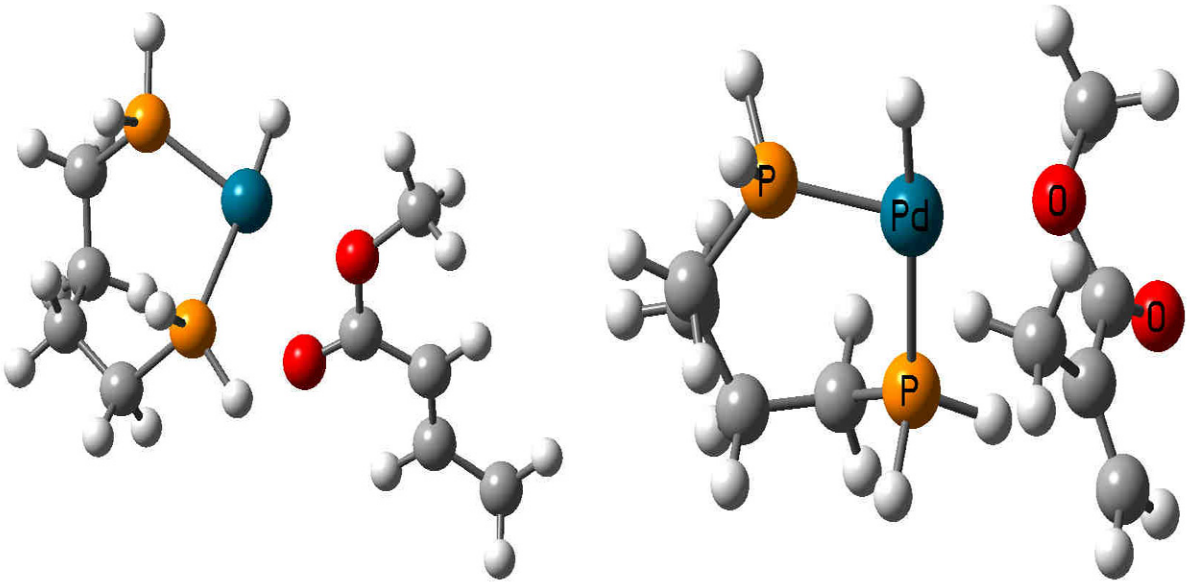

8CT (-2.6 kcal/mol) **8CG (1.3 kcal/mol)**

Figure 10. Optimized structures and relative free energies for intermediates **8CT** and **8CG**.

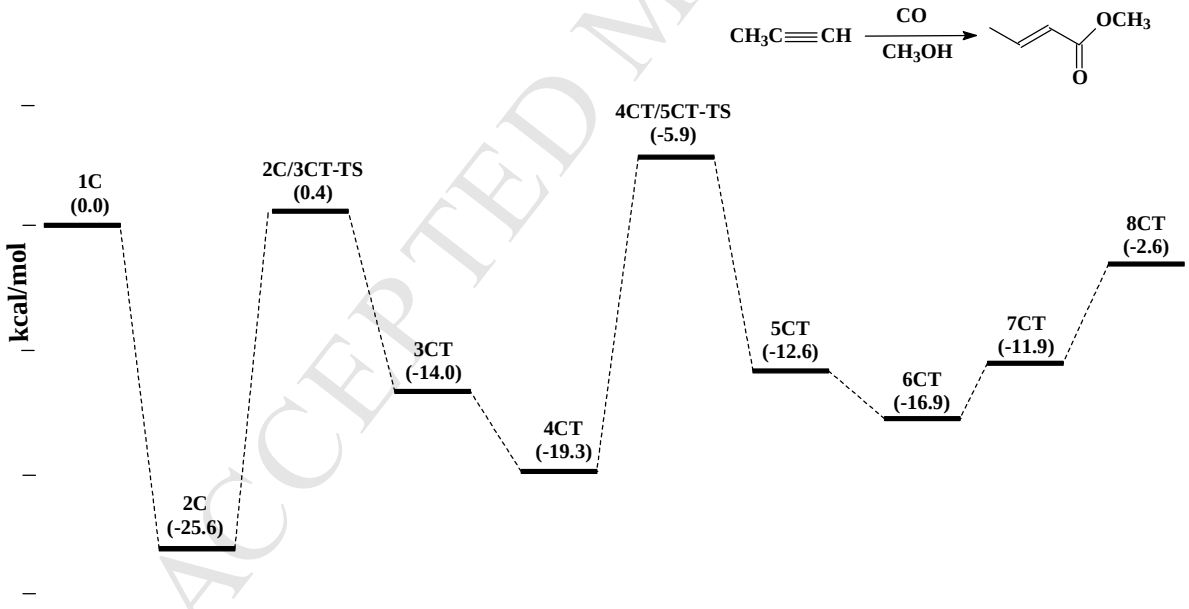

Scheme 2. Computed relative energies (kcal/mol) for the *trans* isomer in gas phase obtained via alkoxycarbonylation of propyne.

Table 1. Total energy difference between *trans* and *gem* intermediates of no ligand simplification in the hydride cycle.

Compound	Energy difference (kcal/mol)*	Energy difference (acetonitrile) (kcal/mol)*
1C-LNS	-	-
2C-LNS	-	-
3CT-LNS	-0.1	-1.6
3CG-LNS		
4CT-LNS	-1.4	-1.6
4CG-LNS		
5CT-LNS	-3.2	-3.6
5CG-LNS		
6CT-LNS	-1.6	-2.3
6CG-LNS		
7CT-LNS	-1.8	-2.3
7CG-LNS		
8CT-LNS	-6.2	-6.4
8CG-LNS		

* Energy difference = E_{tot}(**T**) – E_{tot}(**G**)

Table 2. Comparison of energy profile for all elementary steps involved in the hydride cycle in case of *trans* simplified and non-simplified intermediates.

	E_{tot} (kcal/mol) Simplified intermediates		***E_{tot} (kcal/mol) Non-simplified intermediates***	
	Gas phase	***Acetonitrile***	***Gas phase***	***Acetonitrile***
$HPdP_2$	0	0	0	0
Alkyne coordination	-25.6	-10.2	-17.0	-9.3
Alkyne insertion	-14.9	-17.6	-21.7	-22.2
CO coordination	-19.3	-18.0	-18.7	-16.8
CO insertion	-6.7	-7.6	-9.8	-10.8
Solvent coordination	-16.9	-7.8	-12.1	-7.4
Alcohol coordination	-11.9	-3.8	-7.9	-3.2
Alcohol oxidative addition	-2.6	-0.8	-7.8	-6.6
Product generation	-50.3	-61.9	-50.6	-49.5

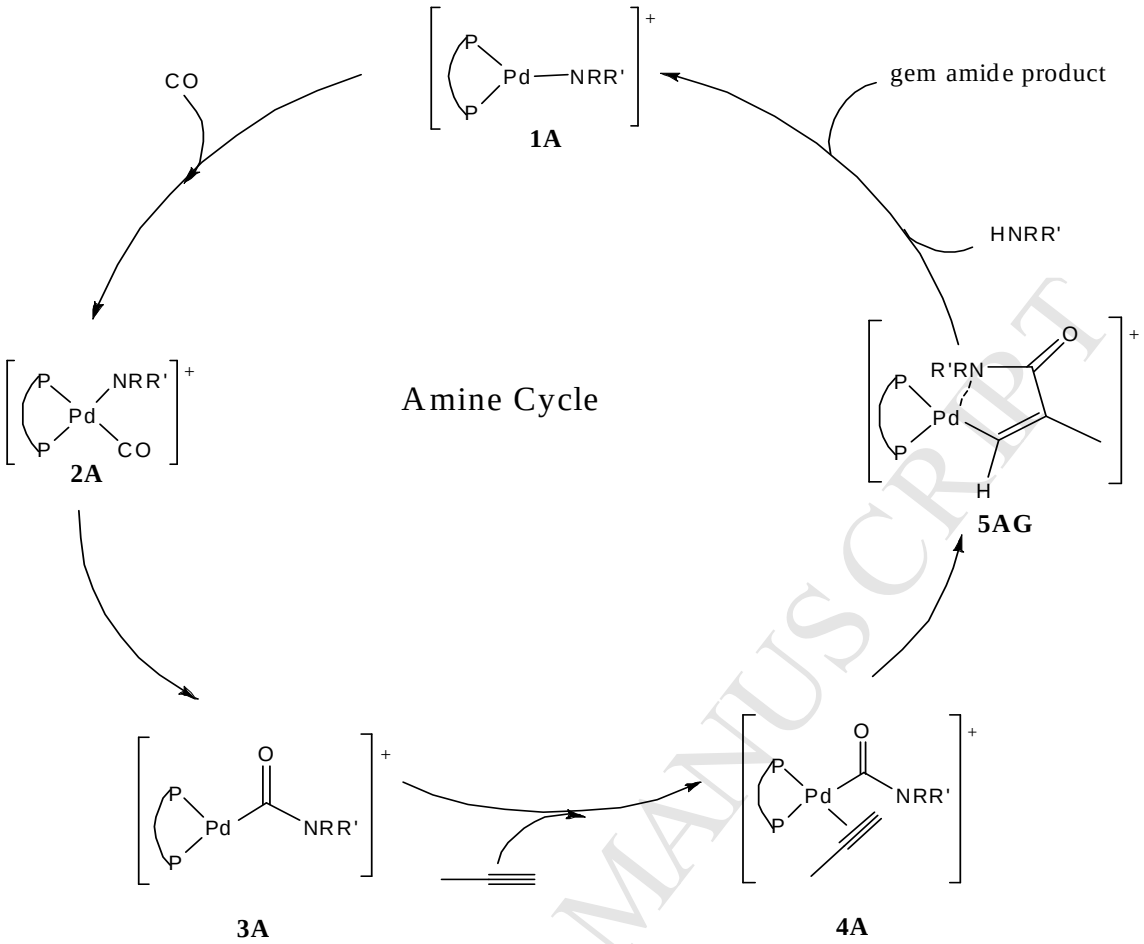

Scheme 3. DFT-derived scheme for aminocarbonylation of propyne by a amine-cationic Palladium(II) bisphosphine complex.

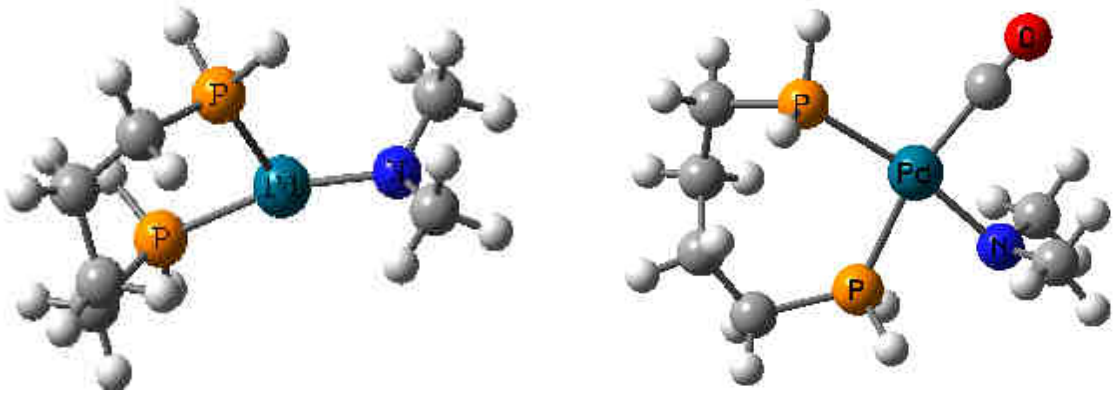

1A (0.0 kcal/mol) **2A (-9.1 kcal/mol)**

Figure 11. Optimized structures and relative free energies for intermediates **1A** and **2A**.

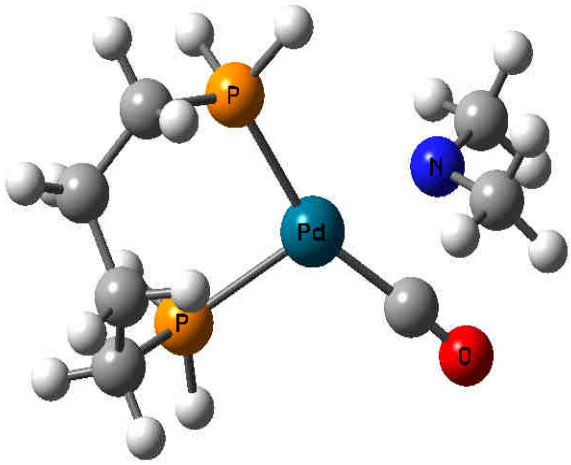

2A/3A-TS (7.6 kcal/mol)

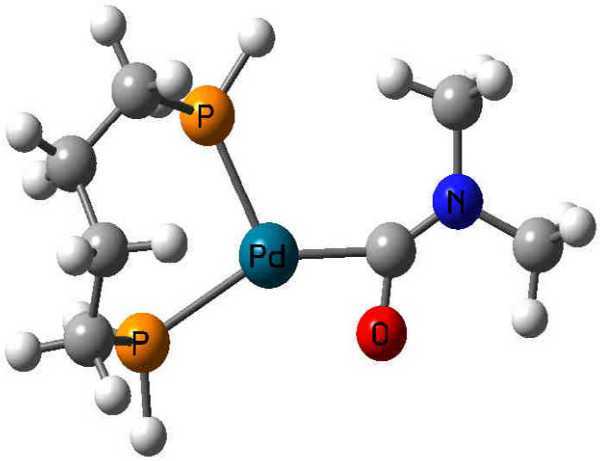

3A (-24.1 kcal/mol)

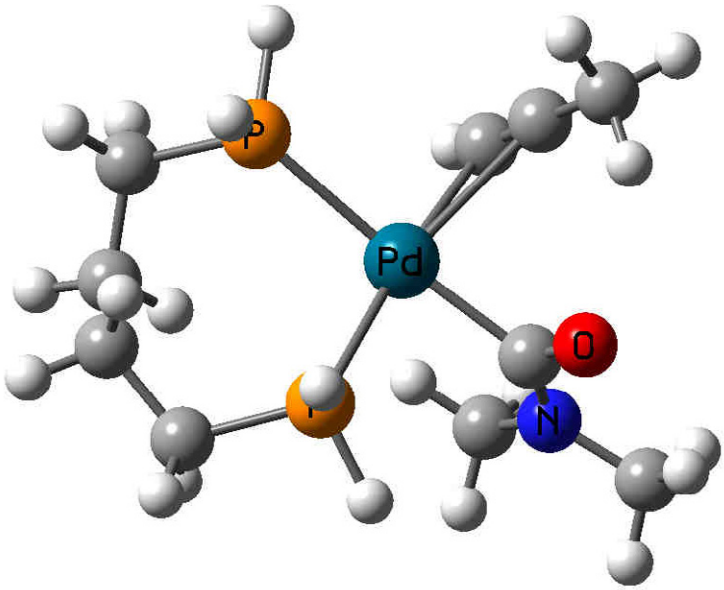

4A (-8.5 kcal/mol)

Figure 12. Optimized structures and relative free energies for transition state **2A/3A-TS** and intermediates, **3A** and **4A**.

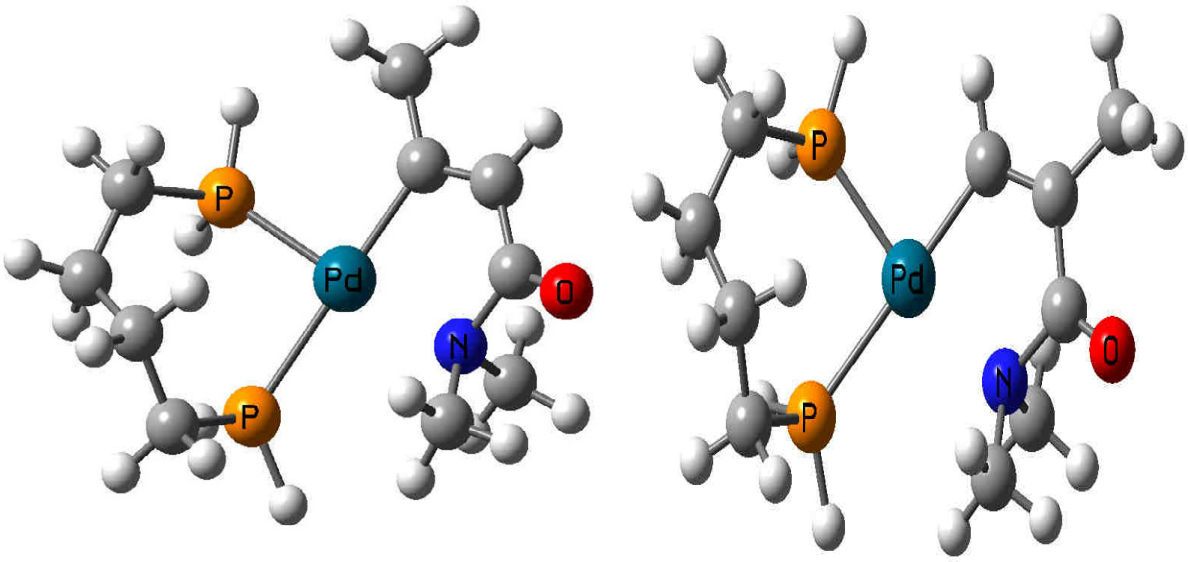

5AT (-18.1 kcal/mol) **5AG (-21.1 kcal/mol)**

Figure 13. Optimized structures and relative free energies for intermediates **5AT** and **5AG**.

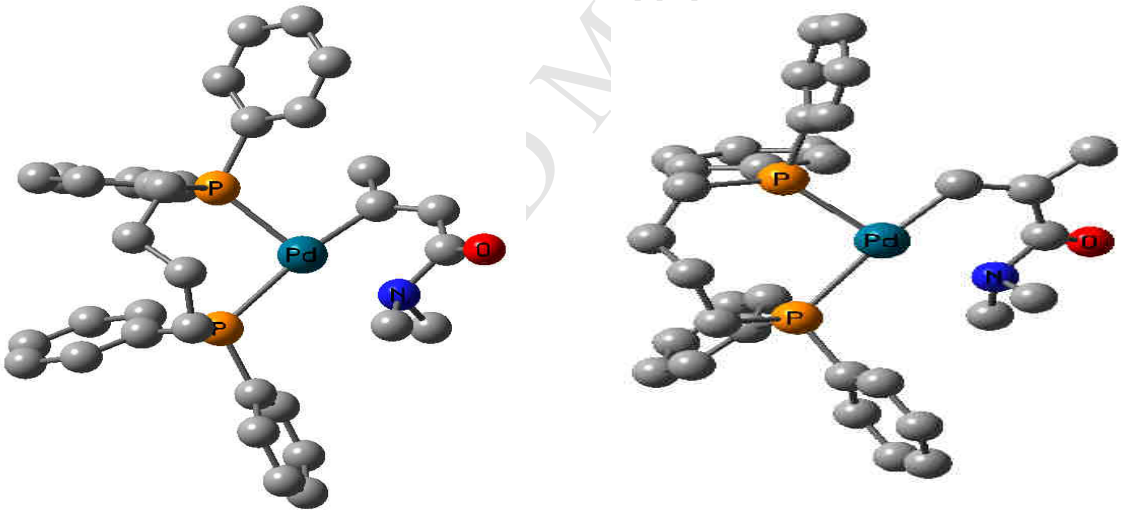

5AT-LNS (E_{tot} = -2257.737852) **5AG-LNS (E_{tot} = -2257.749255)**

Figure 14. Optimized structures and total energies (in au) for intermediates **5AT-LNS** and **5AG-LNS** (H atoms were removed for simplicity).

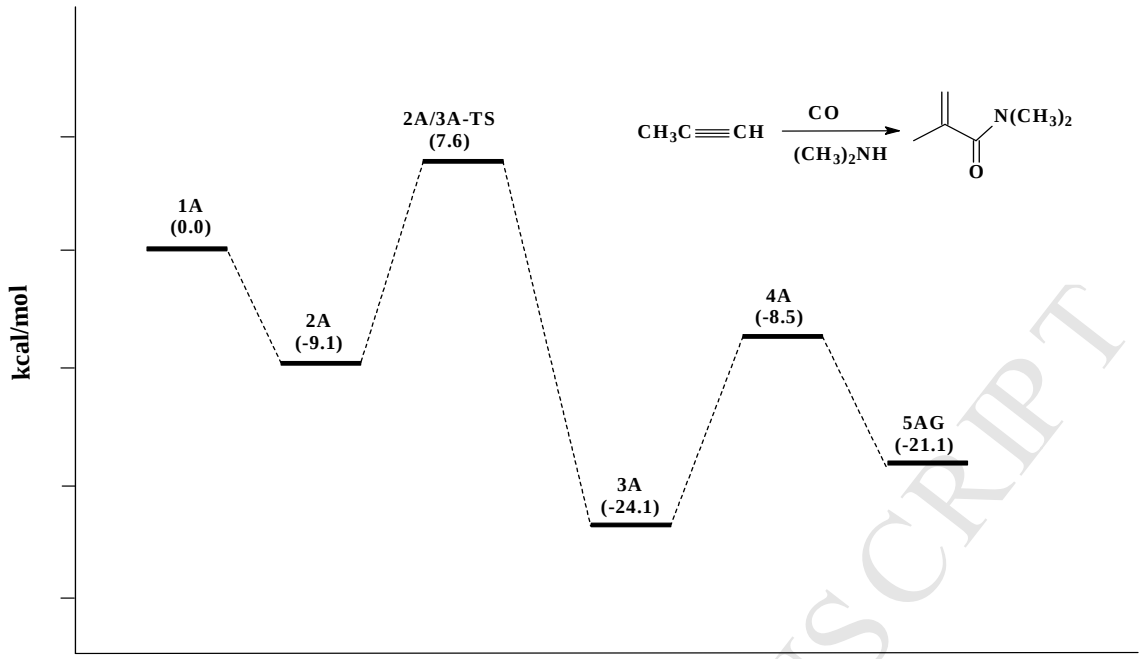

Scheme 4. Computed relative energies (kcal/mol) for the *gem* isomer in gas phase obtained via aminocarbonylation of propyne.

A DFT Study of the Mechanism of Palladium-Catalyzed Alkoxycarbonylation and Aminocarbonylation of Alkynes: Hydride versus Amine Pathways

Rami Suleiman[a], Abdelletif Ibdah[b], and Bassam El Ali[b*]

[a] *Center of Research Excellence in Corrosion, King Fahd University of Petroleum & Minerals (KFUPM), Dhahran 31261, Saudi Arabia*
[b] *Chemistry Department, King Fahd University of Petroleum & Minerals (KFUPM), Dhahran 31261, Saudi Arabia*

Summary:

The difference in activity and regioselectivity of the palladium-catalyzed alkoxycarbonylation and aminocarbonylation of alkynes is studied with the use of DFT computations.

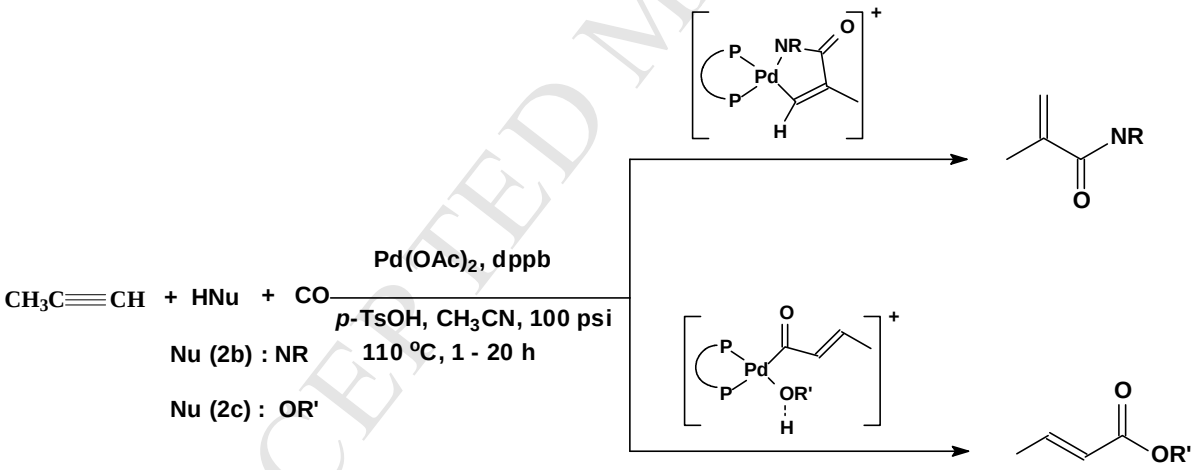

- Palladium-bisphosphine catalyzed alkoxycarbonylation and aminocarbonylation of alkyne (propyne).
- The selectivity towards the *trans* isomer in the alkoxycarbonylation reaction by hydride cycle and to the *gem* isomer in the aminocarbonylation reaction by amine cycle.
- Ligand simplification is not valid in addressing the regioselectivity behavior of alkoxycarbonylation and aminocarbonylation reactions.